Identification of genes potentially involved in bone metastasis by genome-wide gene expression profile analysis of non-small cell lung cancer in mice

LE TAN DAT[1,2], TAISUKE MATSUO[1], TETSURO YOSHIMARU[1], SOJI KAKIUCHI[2], HISATSUGU GOTO[2], MASAKI HANIBUCHI[2], TAKUYA KURAMOTO[1], YASUHIKO NISHIOKA[2], SABURO SONE[2] and TOYOMASA KATAGIRI[1]

[1]Division of Genome Medicine, Institute for Genome Research, The University of Tokushima; [2]Department of Respiratory Medicine and Rheumatology, Institute of Health Biosciences, The University of Tokushima Graduate School, Tokushima 770-8503, Japan

Abstract. Lung cancer is commonly associated with multi-organ metastasis, and the bone is a frequent metastatic site for lung cancer. However, the molecular mechanism of organ-specific metastasis remains poorly understood. To elucidate this issue, we analyzed in this study genome-wide gene expression profiles of 15 metastatic lesions from three organs (bone, lung and liver) in a mouse model with multi-organ metastasis properties of human non-small cell lung cancer cells (ACC-LC319/bone2), using a combination of laser-microbeam microdissection and DNA microarrays. We identified 299 genes that could potentially be involved in the organ-selective nature of lung cancer metastasis. Among them, 77 were bone-specifically expressed elements, including genes involved in cell adhesion, cytoskeleton/cell motility, extracellular matrix remodeling and cell-cell signaling as well as genes already known to be involved in the bone metastasis of breast cancers. Quantitative RT-PCR confirmed the specific upregulation of eight genes in bone metastasis tumors, suggesting that these genes may be involved in bone metastasis. Our findings should be helpful for a better understanding of the molecular aspects of the metastatic process in different organs, and could lead to molecular target-based anticancer drugs and prevention of metastasis, especially bone metastasis.

Introduction

Lung cancer is the leading cause of mortality worldwide and its incidence is rising in many countries (1). The high mortality of this disease is predominantly due to the difficulty of early diagnosis and the highly metastatic potential of lung cancer. In many cases, metastases to multiple organs have already developed by the time of diagnosis (2-4). In particular, ~30-40% of patients with advanced lung cancer will develop bone metastases in the course of their disease, resulting in a significant negative impact on both morbidity and survival (3-5). Currently no curative therapy exists for bone metastasis, and clinical management is generally palliative (3,6,7). Hence, the prevention and treatment of bone metastases are clinically vital.

Most treatments for lung cancer bone metastases are proposed based on targeting the osteoclast-activating pathway, which is the key deregulation in bone metastasis in many types of cancers (3,6-10). However, the cancer cells metastasizing to the bone may express certain features that mediate and favor their colonization in the bone, as well as disrupt the normal balance of bone formation and bone resorption (6,7,9). During such tumor progression, cancer cells are thought to acquire several genetic alterations. We believe that identifying such molecular changes in the cancer cells themselves can probably help to solve, at least in part, bone metastases in lung cancer. In order to understand the molecular mechanism of metastasis, especially bone metastasis, and to establish a molecular-targeted therapy, the development of a clinically relevant animal model is essential. A complex approach of animal models and transcriptomic analyses can provide a considerable amount of information for characterizing the nature of individual cancers; the promise of such information lies in its potential for improving clinical strategies for treatment of cancer through development of novel drugs (5,11,12). With that goal in mind, we performed gene expression profiling in a multiple-organ metastasis mouse model of human small cell lung cancer cells (SCLC), and identified a dozen candidate genes that may affect or determine organ specificity of the metastatic cells, as well as genes involved metastatic processes in different microenvironments (11).

To investigate the molecular bases of organ-specific metastasis, especially the bone, we previously established a multiple-organ metastasis mouse model of human non-small

---

Correspondence to: Dr Toyomasa Katagiri, Division of Genome Medicine, Institute for Genome Research, The University of Tokushima, 3-18-15, Kuramoto-cho, Tokushima 770-8503, Japan
E-mail: tkatagi@genome.tokushima-u.ac.jp

cell lung cancer cells (NSCLC; ACC-LC319/bone2), and performed transcriptomic analysis of *in vivo* metastatic tissues to propose new profiles of lung cancer metastases to multiple organs, including bone metastases. Here, we showed organ-specific gene expression profiles of metastases in the bone, lung and liver, and selectively validated the findings of eight genes in the 'bone profile'. The data from these experiments not only should provide important information about the organ-tropism nature of NSCLC-metastasis, but also be valuable for identifying candidate genes whose products might serve as molecular targets for treatment of NSCLC metastasis, especially bone metastasis.

Materials and methods

Cell lines. A human lung adenocarcinoma cell line ACC-LC-319/bone2 with a high bone metastasis ability was established as described previously (13). We confirmed no *Mycoplasma* contamination in cultures of the cell line used *in vitro* and *in vivo* using PCR Mycoplasma Detection set (Takara, Shiga, Japan). No abnormalities were observed on the cellular morphology of this cell line either at high or low densities of cultures by microscopy. Cells were cultured in RPMI-1640 medium (Invitrogen, Carlsbad, CA), supplemented with 10% fetal bovine serum (Nichirei Biosciences, Tokyo, Japan), antibiotic-antimycotic mixture (Invitrogen), and incubated at 37˚C in a humidified atmosphere containing 5% of CO_2.

In vivo mouse model. Seven-week-old male SCID mice (*C.B-17/ Icr-scid/scidJc1*, CLEA Company, Japan) were depleted of NK-cells and intravenously inoculated with ACC-LC319/bone2 cells as described previously (13). The mice were sacrificed on the 34th day after tumor cell inoculation, and the lungs, livers and hind limp bones containing macroscopic lesions were embedded in Tissue Tek OCT medium (Sakura, Tokyo, Japan), and snap frozen in liquid nitrogen and stored at -80˚C until use. All the experiments in mice were performed under the Guidelines for Animal Welfare in The University of Tokushima, Tokushima.

Laser microbeam microdissection. The frozen tissues were cut into 8-10 μm sections and applied to PEN-membrane slide (Leica, Herborn, Germany), and then stained with hematoxylin and eosin (H&E) for histological examination. The stained tissues were observed microscopically; 15 metastatic lesions (5 bones, 5 lungs and 5 livers) were selectively obtained for laser-microbeam microdissection using PALM Microbeam system (Carl Zeiss, Jena, Germany) according to the manufacturer's protocols. To avoid cross-hybridization of normal mouse mRNA on DNA microarray as described below, we microdissected normal mouse cells in the surrounding regions far from the metastatic lesions of each of the three organs (bone, lung and liver).

RNA extraction, RNA amplification and DNA microarray. Total RNA from each microdissected tissue and the *in vitro* cell line ACC-LC319/bone2 were extracted using RNeasy mini kit (Qiagen, Valencia, CA, USA) according to the manufacturer's protocol. The purity and integrity of RNA were assessed by NanoDrop system (Thermo Scientific, Wilmington, Delaware,

USA) and Agilent RNA 6000 Nano Bioanalyzer (Agilent Technologies), respectively. RNA amplification and labeling of complementary RNA (cRNA) with Cy3 dye were performed using Agilent Low-Input QuickAmp Labeling kit according to the manufacturer's protocol. The Whole Human Genome 4x44K Oligomicroarray kit containing 41,193 probes (60-mer oligo DNA, including control probes) and Gene Expression Hybridization kit were used for the hybridization of labeled RNA. Scanning analysis was performed using the Agilent Microarray scanner and the acquired array images were processed using the Agilent Feature Extractions version 9.5. All the experimental protocols employed followed the manufacturer's protocol (Agilent Technologies).

Microarray data analysis. Microarray data generated by the feature extraction software were loaded in GeneSpring software, version 11.5 (Agilent Technologies). First, we normalized the microarray data across all chips and all genes using quantile normalization, and baseline transformed the signal values to the median in all samples. Then we performed quality control and filtering of the data by flags and by expression level. Entities with flag 'Detected' in at least one out of 18 samples and had values within the 20 and 100th percentiles in at least one out of 18 samples were retained for further analysis.

To identify genes that were differentially expressed among the three types of metastatic tissue, we grouped all five metastases in each of the three organs (bone, lung, liver), and then compared the fold change of expression in one group with the other pool of ten metastases in the other two organs, e.g. five bone metastases would be grouped as 'bone metastases', and compared with the group 'lung and liver metastases' that included five lung metastases and five liver metastases, and so on. We applied random permutation test 10,000 times for each comparison and adjusted for multiple comparison using the Benjamini-Hochberg false discovery rate (FDR). Gene expression level was considered significantly different when FDR was <0.05 (corrected P-value <0.05), and the fold change was at least 2.0 between groups. The output gene lists were further interpreted based on gene ontology analysis.

To rule out the cross-hybridization of normal mouse mRNA to human, we microdissected normal mouse cells from each organ, lung, liver and bone, and hybridized them on human DNA microarrays (Agilent) by the same method as described above. The contamination of mouse genes, if any, most likely had signal intensities above a certain cut-off value. We arbitrarily selected the 95th percentile value of the signal intensities value in metastasis in each organ as the cut-off value, and excluded those genes with signal intensity values higher than this cut-off value in the corresponding normal mouse tissues in each of these three organs.

For hierarchical cluster analysis, the normalized signal intensities of upregulated genes in each organ were subjected to Cluster 3.0 (14), and clustered based on the centroid linkage. The output data were organized using TreeView 1.60 (15). Data from this microarray experiment has been submitted to the NCBI Gene Expression Omnibus (GEO) archive as series GSE29391.

Reverse transcription and real-time RT-PCR. Total RNAs extracted from each of the microdissected tumor samples were

Table I. Primers used in real-time RT-PCR.

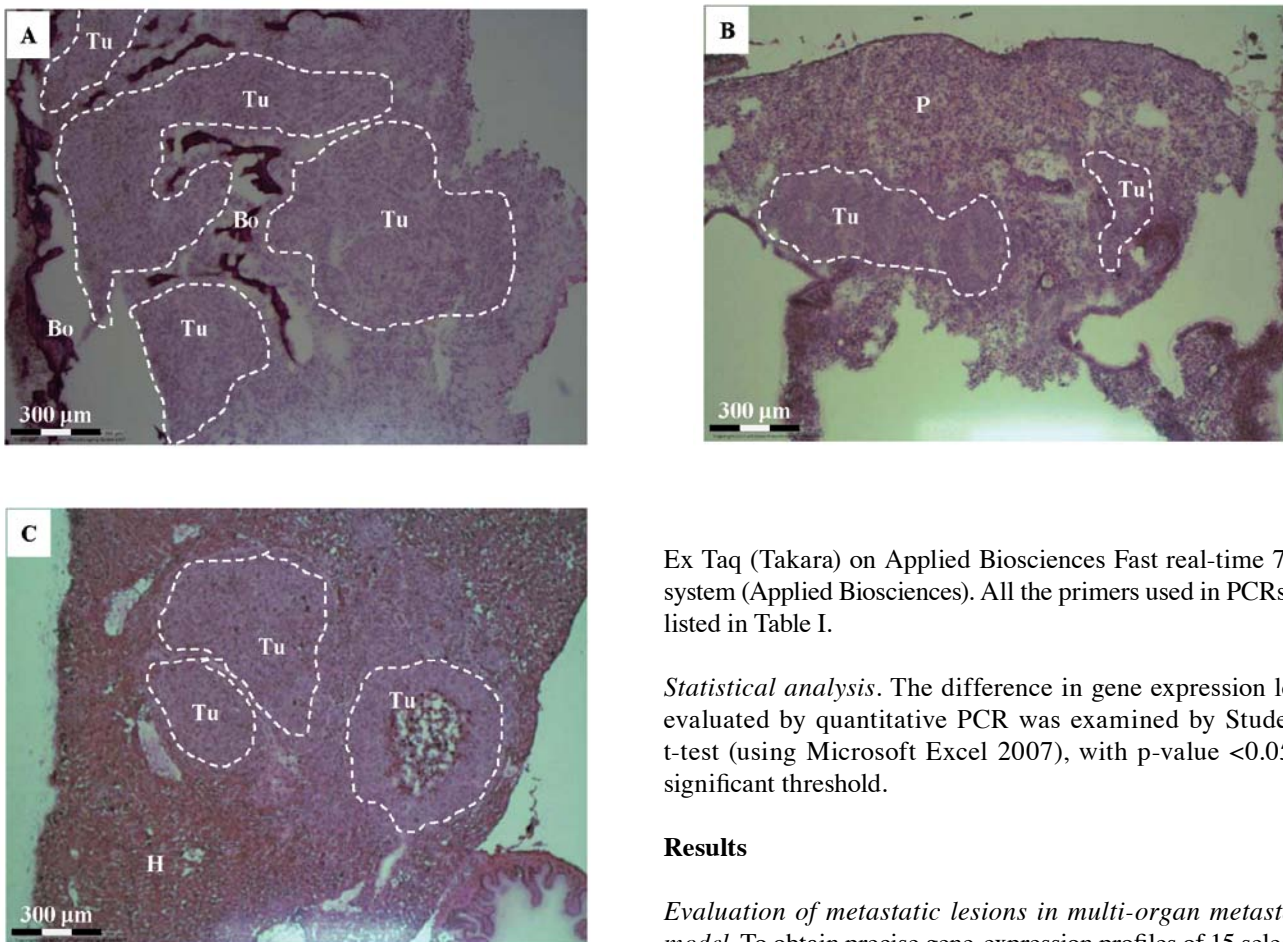| Gene	Fordward primer (5'-3')	Reverse primer (5'-3')
GAPDH	GATCATCAGCAATGCCTCCTG	GAGTCCTTCCACGATACCAAAG
TTYH1	TGTGCTCCCATTTCTGTCCTT	TGCCAGCCCTACTCCCTAGTC
LEFTY1	TTGGGGACTATGGAGCTCAG	TCAAGTCCCTCGATGGCTAC
GUCY1B3	AACAGTGTTTGGCCATGTG	GCTGCCTGTGGTTAATGAG
TM4SF4	GCTTCCTGGCTAACATCCTGTTA	ACACCAGCGCAGGGAAGAT
FOLR1	GTCGACCCTGGAGGAAGAAT	GCCATCTCTCCACAGTGGTT
FGFR3	TCAGGGTGGTCTCTTCTTGG	CGTCGCTGGGTTAACAAAAT
METLL7A	GAGCCCCTAAACATCAAGCA	TTCCAACAGGGGTGGAATTA
CRYM	GAGTGAAACCAGCCCACTGT	TTGGCTGCAACTGTGTCTTC

Figure 1. Histopathology of metastatic lesions in the bone (A), lung (B) and liver (C) (H&E staining). Tu, tumor tissue (dotted area, in some tumors there were necrotic and hemorrhagic regions); H, hepatocyte (normal tissue in liver); P, pneumocyte (normal tissue in lung); Bo, bone (dark area); Scale bars, 300 µm.

reverse-transcribed by SuperScript II reverse-transcriptase (Invitrogen), asccording to the manufacturers protocol. We prepared appropriate dilutions of each single-stranded cDNA for subsequent PCR by monitoring the *glyceraldehyde-3-phosphate dehydrogenase (GAPDH)* as a quantitative internal control. Quantitative PCR were performed using SYBR Premix Ex Taq (Takara) on Applied Biosciences Fast real-time 7500 system (Applied Biosciences). All the primers used in PCRs are listed in Table I.

Statistical analysis. The difference in gene expression level evaluated by quantitative PCR was examined by Student's t-test (using Microsoft Excel 2007), with p-value <0.05 as significant threshold.

Results

Evaluation of metastatic lesions in multi-organ metastasis model. To obtain precise gene-expression profiles of 15 selected metastatic lesions (five in each organ: lung, liver, and bone) in a mouse model, we purified cancer cells from each organ by laser-microbeam microdissection (see Materials and methods). The representative histopathological features of each of metastatic lesions in bone, lung and liver are shown in Fig. 1. Consistent with previous results (13), all mice developed metastases in bones as evaluation by overt clinical signs, sick mice showed limping due to fractures of hind limps, together with other signs such as weight loss, ruffling fur, dyspnea, big belly, but we collected osteolytic lesions in this microarray analysis because osteoblastic lesions were observed to a much lesser extent (~30%) (Fig. 1A). We also observed metastatic lesions in lungs and livers of all mice (Fig. 1B and C).

Table II. Bone metastasis gene expression profile of upregulated genes with FC >2.0, and P-value <0.05.

Gene symbol	Accession number	Gene name	P-value	Fold change
Cell adhesion				
SNED1	NM_001080437	Sushi, nidogen and EGF-like domains 1	<0.001	2.494
TTYH1	NM_020659	Tweety homolog 1 *(Drosophila)*	0.016	2.374
GPR98	AL136541	G protein-coupled receptor 98	0.047	2.110
SPON2	NM_012445	Spondin 2, extracellular matrix protein	0.020	2.029
Cytoskeleton/cell motility				
MYL1	NM_079420	Myosin, light chain 1, alkali; skeletal, fast	0.020	5.571
TNNI2	NM_003282	Troponin I type 2 (skeletal, fast)	0.036	5.211
MYO1A	NM_005379	Myosin IA	0.025	2.677
TTLL6	NM_173623	Tubulin tyrosine ligase-like family, member 6	<0.001	2.570
Extracellular matrix remodeling				
COL8A1	NM_001850	Collagen, type VIII, α1	0.020	2.933
COL6A3	NM_004369	Collagen, type VI, α3	0.016	2.246
Cell-cell signaling (cytokine/chemokine)				
LEFTY1	NM_020997	Left-right determination factor 1	0.020	2.836
CDNF	NM_001029954	Cerebral dopamine neurotrophic factor	0.020	2.654
CHIA	NM_021797	Chitinase, acidic	0.046	2.302
Signal transduction				
PPP1R1B	NM_032192	Protein phosphatase 1, regulatory (inhibitor) subunit 1B	0.016	3.376
GUCY1B3	NM_000857	Guanylate cyclase 1, soluble, β3	0.020	2.613
DOK7	NM_173660	Docking protein 7	0.046	2.463
TM4SF4	NM_004617	Transmembrane 4 L six family member 4	0.032	2.429
PTPRD	NM_002839	Protein tyrosine phosphatase, receptor type, D	0.011	2.222
ARHGAP29	BC022483	Rho GTPase activating protein 29	0.016	2.211
FOLR1	NM_016725	Folate receptor 1 (adult)	0.020	2.178
CLEC11A	NM_002975	C-type lectin domain family 11, member A	0.010	2.101
FGFR3	NM_000142	Fibroblast growth factor receptor 3, variant 1	0.013	2.071
Immune response				
POU2AF1	NM_006235	POU class 2 associating factor 1	0.010	4.962
PLA2G1B	NM_000928	Phospholipase A2, group IB (pancreas)	0.016	2.298
RNF125	AK027134	Ring finger protein 125	0.016	2.076
Metabolism/catalytic activity				
PNMT	NM_002686	Phenylethanolamine N-methyltransferase	0.020	3.681
C3orf57	NM_001040100	Chromosome 3 open reading frame 57	0.010	3.361
ECHDC3	NM_024693	Enoyl Coenzyme A hydratase domain containing 3	0.010	3.086
CTSO	NM_001334	Cathepsin O	0.032	2.766
NUDT7	NM_001105663	Nudix (nucleoside diphosphate linked moiety X)-type motif 7	0.024	2.617
METTL7A	NM_014033	Methyltransferase like 7A	0.015	2.420
ADPRHL1	NM_138430	ADP-ribosylhydrolase like 1	<0.001	2.370
PACSIN1	NM_020804	Protein kinase C and casein kinase substrate in neurons 1	0.015	2.250
GPIHBP1	NM_178172	Glycosylphosphatidylinositol anchored high density lipoprotein binding protein 1	0.020	2.210
FMO5	NM_001461	Flavin containing monooxygenase 5	0.038	2.178
PACSIN1	NM_020804	Protein kinase C and casein kinase substrate in neurons 1	0.016	2.160
CRYM	NM_001888	Crystallin, mu	0.040	2.131
STK31	NM_032944	Serine/threonine kinase 31	0.032	2.066
MDH1B	BC033509	Malate dehydrogenase 1B, NAD (soluble)	0.032	2.054
SPTLC3	NM_018327	Serine palmitoyltransferase, long chain base subunit 3	0.016	2.010

Table II. Continued.

Gene symbol	Accession number	Gene name	P-value	Fold change
Cell cycle, apoptosis				
DAPL1	NM_001017920	Death associated protein-like 1	0.010	9.621
PLK1S1	BC039296	Polo-like kinase 1 substrate 1	0.021	2.216
Transcription				
N/A	AF023203	Homeobox protein Og12 (OGL12)	0.020	8.619
Transporter activity				
CACNG7	NM_031896.4	Calcium channel, voltage-dependent, gamma subunit 7	0.010	5.516
ATP2A1	NM_173201	ATPase, Ca^{2+} transporting, cardiac muscle, fast twitch 1	0.013	5.210
CCT6B	NM_006584	Chaperonin containing TCP1, subunit 6B (ζ2)	0.016	3.507
SLC16A14	NM_152527	Solute carrier family 16, member 14 (monocarboxylic acid transporter 14)	0.024	2.952
SLC5A9	NM_001011547	Solute carrier family 5 (sodium/glucose cotransporter), member 9	0.032	2.377
SLC23A1	NM_152685	Solute carrier family 23 (nucleobase transporters), member 1	0.032	2.290
SLC16A14	NM_152527	Solute carrier family 16, member 14 (monocarboxylic acid transporter 14)	0.017	2.050
ABCD3	NM_002858	ATP-binding cassette, sub-family D (ALD), member 3	0.016	2.034
GLTPD2	NM_001014985	Glycolipid transfer protein domain containing 2	0.015	2.027
Calcium ion binding				
EFHC2	NM_025184	EF-hand domain (C-terminal) containing 2	0.015	4.518
EFHB	NM_144715	EF-hand domain family, member B	0.040	2.392
ANXA13	NM_001003954	Annexin A13	0.029	2.108
The others				
ITM2A	NM_004867	Integral membrane protein 2A	0.011	4.216
APCDD1L	NM_153360	Adenomatosis polyposis coli down-regulated 1-like	0.047	4.034
RSPH1	NM_080860	Radial spoke head 1 homolog (Chlamydomonas)	0.010	3.300
NEB	NM_004543	Nebulin	0.015	2.603
DENND1B	AL831839	DENN/MADD domain containing 1B	0.032	2.011
Unknown				
C17orf108	NM_001076680	Chromosome 17 open reading frame 108	0.010	4.160
C11orf93	NM_001136105	Chromosome 11 open reading frame 93	0.010	3.023
UNQ1944	AY358202	RVLA1944	0.044	2.704
DENND2C	CR749576	DENN/MADD domain containing 2C	0.025	2.700
FAM167A	NM_053279	Family with sequence similarity 167, member A	0.037	2.666
PRY2	NM_001002758	PTPN13-like, Y-linked 2	0.030	2.598
C11orf92	NM_207429	Chromosome 11 open reading frame 92	0.015	2.554
N/A	AL833005		0.016	2.465
REEP2	NM_016606	Receptor accessory protein 2	0.010	2.319
C17orf108	BC042947	Chromosome 17 open reading frame 108	0.034	2.300
N/A	AK023574		0.040	2.253
C16orf73	NM_152764	Chromosome 16 open reading frame 73	0.017	2.214
N/A	AJ412029		0.016	2.161
N/A	AL834280		0.047	2.141
N/A	AK055981		0.010	2.121
RPL27A	NM_000990	Ribosomal protein L27a	0.047	2.061
N/A	AX748211		0.020	2.000

P-value, Benjamini-Hochberg false discovery rate of random permutation test; Fold change, ratio of gene expression levels between groups. Gene symbol, accession number, gene name: exported from GeneSpring (from the NCBI databases). FC, fold change; N/A, not available. In each gene ontology functional term, genes were ranked according to fold change (highest to lowest).

Table III. Lung metastasis gene expression profile of upregulated genes with FC >2.0, and P-value <0.05.

Gene symbol	Accession number	Gene name	P-value	Fold change
Cell adhesion				
CLDN18	NM_016369	Claudin 18	0.003	20.878
FLRT3	NM_198391	Fibronectin leucine rich transmembrane protein 3	0.003	6.880
IGFBP7	NM_001553	Insulin-like growth factor binding protein 7	0.005	5.166
ALCAM	NM_001627	Activated leukocyte cell adhesion molecule	0.003	3.882
LRRN2	NM_201630	Leucine rich repeat neuronal 2	0.003	3.790
PTPRF	NM_002840	Protein tyrosine phosphatase, receptor type, F	0.010	2.885
SRPX	NM_006307	Sushi-repeat-containing protein, X-linked	0.031	2.510
PVRL3	BC017572	Poliovirus receptor-related 3	0.003	2.509
PVRL3	NM_015480	Poliovirus receptor-related 3	0.003	2.477
CGN	NM_020770	Cingulin	0.019	2.472
PVRL3	BC017572	Poliovirus receptor-related 3	0.009	2.462
F5	NM_000130	Coagulation factor V (proaccelerin, labile factor)	0.042	2.418
DDR2	NM_001014796	Discoidin domain receptor tyrosine kinase 2	0.048	2.353
NRP2	NM_018534	Neuropilin 2 (variant 4)	0.003	2.348
ITGB2	NM_000211	Integrin, β2 (complement component 3 receptor 3 and 4 subunit)	0.023	2.338
NRP2	NM_201266	Neuropilin 2 (variant 1)	0.030	2.078
STAB1	NM_015136	Stabilin 1	0.003	2.027
Cytoskeleton/cell motility				
SHROOM3	NM_020859	Shroom family member 3	0.008	8.364
NTN1	NM_004822	Netrin 1	0.014	3.064
KRT80	NM_182507	Keratin 80	0.014	2.544
Extracellular matrix remodeling				
SFTPC	NM_003018	Surfactant protein C	0.003	191.604
SFTPD	NM_003019	Surfactant protein D	0.003	94.641
GPC3	NM_004484	Glypican 3	0.037	6.034
CHI3L1	NM_001276	Chitinase 3-like 1 (cartilage glycoprotein-39)	0.014	5.513
COL4A3	NM_000091	Collagen, type IV, α3 (Goodpasture antigen)	0.047	4.716
TGFBI	NM_000358	Transforming growth factor, β-induced, 68 kDa	0.007	3.301
COL1A1	Z74615	Collagen, type I, α1	0.007	2.657
BMP5	NM_021073	Bone morphogenetic protein 5	0.034	2.443
CPM	NM_001874	Carboxypeptidase M	0.023	2.233
MATN2	NM_030583	Matrilin 2	0.014	2.190
VCAN	NM_004385	Versican	0.038	2.156
Cell-cell signaling (cytokine/chemokine)				
IGF2	NM_000612	Insulin-like growth factor 2 (somatomedin A)	0.003	6.449
PRICKLE1	NM_153026	Prickle homolog 1 (*Drosophila*)	0.003	5.549
TCN1	NM_001062	Transcobalamin I (vitamin B12 binding protein, R binder family)	0.016	4.445
CAMP	NM_004345	Cathelicidin antimicrobial peptide	0.010	4.118
PHLDB2	NM_145753	Pleckstrin homology-like domain, family B, member 2	0.014	4.056
NTN4	NM_021229	Netrin 4	0.003	3.243
FSTL1	NM_007085	Follistatin-like 1	0.019	2.893
PRRG3	NM_024082	Proline rich Gla (G-carboxyglutamic acid) 3 (transmembrane)	0.049	2.838
NTN4	NM_021229	Netrin 4	0.003	3.243
FSTL1	NM_007085	Follistatin-like 1	0.019	2.893
PRRG3	NM_024082	Proline rich Gla (G-carboxyglutamic acid) 3 (transmembrane)	0.049	2.838
PRRG3	NM_024082	Proline rich Gla (G-carboxyglutamic acid) 3 (transmembrane)	0.049	2.838
NTNG1	NM_014917	Netrin G1	0.008	2.815
RSPO3	NM_032784	R-spondin 3 homolog (*Xenopus laevis*)	0.023	2.348

Table III. Continued.

Gene symbol	Accession number	Gene name	P-value	Fold change
INHBB	NM_002193	Inhibin, βB	0.022	2.181
Signal transduction				
DKK1	NM_012242	Dickkopf homolog 1 (*Xenopus laevis*)	0.003	11.313
RICH2	NM_014859	Rho-type GTPase-activating protein RICH2	0.003	11.012
IL7R	NM_002185	Interleukin 7 receptor	0.009	7.874
PDGFRA	NM_006206	Platelet-derived growth factor receptor, α polypeptide	0.003	5.941
CDC42EP3	AK055915	CDC42 effector protein (Rho GTPase binding) 3	0.003	5.133
CDC42EP3	NM_006449	CDC42 effector protein (Rho GTPase binding) 3	0.003	4.854
GRIA3	NM_000828	Glutamate receptor, ionotrophic, AMPA 3	0.023	4.328
AFAP1L2	NM_001001936	Actin filament associated protein 1-like 2	0.014	4.202
TGFB2	NM_001135599	Transforming growth factor, β2	0.008	4.098
DPYSL5	NM_020134	Dihydropyrimidinase-like 5	0.007	3.537
MX1	NM_002462	Myxovirus (influenza virus) resistance 1, interferon-inducible protein p78 (mouse)	0.036	3.304
STMN2	S82024	Stathmin-like 2	0.023	3.237
CFI	NM_000204	Complement factor I	0.008	3.036
PTPRB	NM_002837	Protein tyrosine phosphatase, receptor type, B	0.016	2.919
SEMA7A	NM_003612	Semaphorin 7A, GPI membrane anchor (John Milton Hagen blood group)	0.034	2.825
SOCS2	NM_003877	Suppressor of cytokine signaling 2	0.026	2.712
CFI	NM_000204	Complement factor I	0.042	2.603
IRS1	NM_005544	Insulin receptor substrate 1	0.016	2.403
LTBP1	NM_206943	Latent transforming growth factor β binding protein 1	0.041	2.393
PRKG1	NM_006258	Protein kinase, cGMP-dependent, type I	0.016	2.334
RTKN2	NM_145307	Rhotekin 2	0.022	2.287
AKAP12	NM_005100	A kinase (PRKA) anchor protein 12	0.023	2.280
RASGRP2	NM_153819	RAS guanyl releasing protein 2 (calcium and DAG-regulated)	0.044	2.228
GPR124	NM_032777	G protein-coupled receptor 124	0.041	2.202
IL17RD	NM_017563	Interleukin 17 receptor D	0.016	2.162
RTKN2	BC025765	Rhotekin 2	0.038	2.158
QKI	NM_206855	Quaking homolog, KH domain RNA binding (mouse)	0.003	2.054
THBD	NM_000361	Thrombomodulin	0.022	2.013
Immune response				
PBX1	NM_002585	Pre-B-cell leukemia homeobox 1	0.013	3.229
NCF2	NM_000433	Neutrophil cytosolic factor 2	0.044	3.151
TLR4	NM_138554	Toll-like receptor 4	0.038	2.518
ANXA3	NM_005139	Annexin A3	0.024	2.217
B2M	NM_004048	β-2-microglobulin	0.022	2.217
JAG2	NM_002226	Jagged 2	0.016	2.049
Metabolism				
ALDH1A2	NM_170697	Aldehyde dehydrogenase 1 family, member A2	0.005	6.147
CYP24A1	NM_000782	Cytochrome P450, family 24, subfamily A, polypeptide 1	0.009	5.172
LIPG	NM_006033	Lipase, endothelial	0.016	3.961
CYP24A1	NM_000782	Cytochrome P450, family 24, subfamily A, polypeptide 1	0.003	3.480
MGAT3	NM_002409	Mannosyl (β-1,4-)-glycoprotein β-1, 4-N-acetylglucosaminyltransferase	0.019	3.420
ME1	L34035	Malic enzyme 1, NADP(+)-dependent, cytosolic	0.022	3.344
GDA	NM_004293	Guanine deaminase	0.022	2.956
MGAT5B	NM_144677	Mannosyl (α-1,6-)-glycoprotein β-1, 6-N-acetyl-glucosaminyltransferase, isozyme B	0.033	2.783
ADAM19	NM_033274	ADAM metallopeptidase domain 19 (meltrin β)	0.005	2.212
ALPK2	NM_052947	α-kinase 2	0.028	2.181
PLTP	NM_006227	Phospholipid transfer protein	0.005	2.040

Table III. Continued.

Gene symbol	Accession number	Gene name	P-value	Fold change
ARG2	NM_001172	Arginase, type II	0.033	2.007
CHST8	NM_022467	Carbohydrate (N-acetylgalactosamine 4-0) sulfotransferase 8	0.038	2.006
Cell cycle, apoptosis				
SULF1	NM_015170	Sulfatase 1	0.034	4.318
LCN2	NM_005564	Lipocalin 2	0.013	3.799
LYZ	NM_000239	Lysozyme (renal amyloidosis)	0.003	2.940
SGK1	NM_005627	Serum/glucocorticoid regulated kinase 1	0.027	2.329
CCND2	NM_001759	Cyclin D2	0.005	2.088
Transcription				
IRX2	NM_033267	Iroquois homeobox 2	0.005	33.528
BHLHE22	NM_152414	Basic helix-loop-helix family, member e22	0.003	6.219
HOPX	NM_139211	HOP homeobox	0.003	4.453
NFE4	BC036938	Transcription factor NF-E4	0.023	3.860
NKX2-1	NM_003317	NK2 homeobox 1	0.013	3.341
HIC1	NM_006497	Hypermethylated in cancer 1	0.003	2.818
IKZF2	NM_001079526	IKAROS family zinc finger 2 (Helios)	0.014	2.441
KLF2	NM_016270	Kruppel-like factor 2 (lung)	0.003	2.199
ETS2	NM_005239	V-ets erythroblastosis virus E26 oncogene homolog 2 (avian)	0.005	2.183
BACH2	NM_021813	BTB and CNC homology 1, basic leucine zipper transcription factor 2	0.005	2.159
MEIS1	NM_002398	Meis homeobox 1	0.033	2.005
Transporter activity				
SLC35F3	NM_173508	Solute carrier family 35, member F3	0.003	5.060
MAL2	NM_052886	Mal, T-cell differentiation protein 2	0.041	3.569
RBP1	NM_002899	Retinol binding protein 1, cellular	0.017	2.765
SLC16A2	NM_006517	Solute carrier family 16, member 2 (monocarboxylic acid transporter 8)	0.005	2.763
RHCG	NM_016321	Rh family, C glycoprotein	0.007	2.350
UCP2	NM_003355	Uncoupling protein 2 (mitochondrial, proton carrier)	0.003	2.074
Others				
LIMCH1	NM_014988	LIM and calponin homology domains 1	0.003	23.809
BICC1	AK130049	Bicaudal C homolog 1 (*Drosophila*)	0.013	6.773
SHISA9	NM_001145205	Shisa homolog 9 (*Xenopus laevis*)	0.003	6.281
VSIG2	NM_014312	V-set and immunoglobulin domain containing 2	0.015	4.631
CELF4	NM_020180	CUGBP, Elav-like family member 4	0.008	4.248
ZNF365	NM_014951	Zinc finger protein 365	0.024	3.504
SETBP1	NM_015559	SET binding protein 1	0.013	3.469
C11orf41	NM_012194	Chromosome 11 open reading frame 41	0.003	3.278
ZNF608	NM_020747	Zinc finger protein 608	0.009	3.272
SERTAD4	NM_019605	SERTA domain containing 4	0.008	3.104
SUSD4	NM_017982	Sushi domain containing 4	0.034	3.044
LYPD1	NM_144586	LY6/PLAUR domain containing 1	0.043	3.033
FRMD5	NM_032892	FERM domain containing 5	0.013	3.007
HBA1	NM_000558	Hemoglobin, α1	0.044	3.000
HBA2	NM_000517	Hemoglobin, α2	0.043	2.993
MAP1LC3A	NM_032514	Microtubule-associated protein 1 light chain 3α	0.035	2.495
CELF2	NM_001025077	CUGBP, Elav-like family member 2	0.005	2.458
SPANXA1	NM_013453	Sperm protein associated with the nucleus, X-linked, family member A1	0.023	2.445
SPANXD	NM_032417	SPANX family, member D	0.030	2.370
SUSD4	NM_001037175	Sushi domain containing 4	0.022	2.206

Table III. Continued.

Gene symbol	Accession number	Gene name	P-value	Fold change
MAN1A1	NM_005907	Mannosidase, alpha, class 1A, member 1	0.019	2.200
MTUS2	NM_001033602	Microtubule associated tumor suppressor candidate 2	0.023	2.200
ATAD3B	AB033099	ATPase family, AAA domain containing 3B	0.013	2.178
PMEPA1	NM_020182	Prostate transmembrane protein, androgen induced 1	0.003	2.163
FILIP1L	NM_182909	Filamin A interacting protein 1-like	0.023	2.080
FAM20A	NM_017565	Family with sequence similarity 20, member A	0.009	2.043
C1QL1	NM_006688	Complement component 1, q subcomponent-like 1	0.045	2.027
Unknown				
N/A	AK054921		0.013	10.114
N/A	AB025028		0.041	6.451
N/A	BC040881		0.007	5.805
N/A	AK125437		0.008	5.127
N/A	CA314451		0.017	4.233
N/A	AK023954		0.019	3.543
H19	NR_002196	H19, imprinted maternally expressed transcript (non-protein coding)	0.049	3.263
C1orf133	NR_024337	Chromosome 1 open reading frame 133	0.016	2.819
PIK3IP1	NM_052880	Phosphoinositide-3-kinase interacting protein 1	0.046	2.776
FAM117A	NM_030802	Family with sequence similarity 117, member A	0.003	2.669
KIAA1199	NM_018689	KIAA1199	0.013	2.643
N/A	AI754733		0.010	2.606
N/A	BX097190		0.016	2.540
C12orf53	NM_153685	Chromosome 12 open reading frame 53	0.017	2.530
N/A	AK098514		0.047	2.346
N/A	BC041955		0.014	2.340
N/A	AK024680		0.005	2.329
CCDC79	NM_001136505	Coiled-coil domain containing 79	0.044	2.324
N/A	R78584		0.015	2.254
HLA-L	NR_027822	Major histocompatibility complex, class I, L, pseudogene	0.012	2.171
N/A	AK025975		0.012	2.131
N/A	AI161396		0.007	2.120
HCG26	NR_002812	HLA complex group 26 (non-protein coding)	0.046	2.115
N/A	BY798802		0.037	2.109
SPOCD1	NM_144569	SPOC domain containing 1	0.008	2.091
N/A	AA731781		0.023	2.087
PANX2	NM_052839	Pannexin 2	0.024	2.062
N/A	AK296148		0.047	2.039

P-value, Benjamini-Hochberg false discovery rate of random permutation test; Fold change, ratio of gene expression levels between groups. Gene symbol, accession number, gene name: exported from GeneSpring (from the NCBI databases). FC, fold change; N/A, not available. In each gene ontology functional term, genes were ranked according to fold change (highest to lowest).

Up- and downregulated gene expression profile of organ-selective metastases. To identify genes that were selectively expressed in each of the three metastatic organs, we performed the fold-change analysis in accordance with the following criteria: genes that were differentially expressed by at least two-fold with $P < 0.05$ in one metastatic organ as compared to metastases in the other two organs. We identified a total of 299 genes, which were potentially involved in multi-organ-metastasis features of lung cancer, including the upregulated genes in bone (77 genes), lung (106 genes) and liver (56 genes) metastases (Tables II-IV). Moreover, a hierarchical clustering

analysis of these 299 upregulated genes using Cluster and TreeView (14,15) obviously separated the three-organ-specific groups of metastatic lesions (Fig. 2A). The genes preferentially expressed in bone metastases were shown as the focused view of the dendrogram (Fig. 2B).

Validation of bone-preferentially expressed genes. To validate the reliability of the expression data obtained by microarray analysis, we performed quantitative RT-PCR for eight genes that were preferentially overexpressed in bone metastasis. The results confirmed the microarray data in all of the tumors tested

Table IV. Liver metastasis gene expression profile of upregulated genes with FC >2.0, and P-value <0.05.

Gene symbol	Accession number	Gene name	P-value	Fold change
Cell adhesion				
VTN	NM_000638	Vitronectin	0.005	57.713
APOA4	NM_000482	Apolipoprotein A-IV	0.015	32.078
KNG1	NM_000893	Kininogen 1	0.005	11.411
DPP4	NM_001935	Dipeptidyl-peptidase 4	0.007	2.174
Extracellular matrix remodeling				
SOD3	NM_003102	Superoxide dismutase 3, extracellular	0.046	2.797
ZG16B	NM_145252	Zymogen granule protein 16 homolog B (rat)	0.013	2.330
Cell-cell signaling (cytokine/chemokine)				
HGFAC	NM_001528	HGF activator	0.009	4.183
C4orf7	NM_152997	Chromosome 4 open reading frame 7	0.027	3.725
STC1	NM_003155	Stanniocalcin 1	0.013	2.958
DACT1	NM_016651	Dapper, antagonist of β-catenin, homolog 1 (*Xenopus laevis*)	0.045	2.592
STC2	NM_003714	Stanniocalcin 2	0.048	2.222
Signal transduction				
APOA1	NM_000039	Apolipoprotein A-I	0.005	63.590
DHCR24	NM_014762	24-Dehydrocholesterol reductase	0.005	3.597
PITPNC1	AK094724	Phosphatidylinositol transfer protein, cytoplasmic 1	0.034	3.319
PITPNC1	NM_181671	Phosphatidylinositol transfer protein, cytoplasmic 1	0.023	2.551
SORL1	NM_003105	Sortilin-related receptor, L(DLR class) A repeats-containing	0.009	2.455
CALCR	NM_001742	Calcitonin receptor	0.045	2.385
ANGPTL4	NM_139314	Angiopoietin-like 4	0.043	2.075
Immune response				
NDRG1	NM_006096	N-myc downstream regulated 1	0.005	2.073
Cell cycle, apoptosis				
KLK10	NM_002776	Kallikrein-related peptidase 10	0.005	18.807
GAS2	NM_005256	Growth arrest-specific 2	0.014	6.565
Transcription				
ONECUT2	NM_004852	One cut homeobox 2	0.025	4.084
MLXIPL	NM_032951	MLX interacting protein-like	0.050	2.436
HIF3A	NM_022462	Hypoxia inducible factor 3, α subunit	0.014	2.356
TMEM229A	NM_001136002	Transmembrane protein 229A	0.047	2.220
PPARGC1A	NM_013261	Peroxisome proliferator-activated receptor γ, coactivator 1α	0.027	2.039
Metabolism				
CPS1	NM_001875	Carbamoyl-phosphate synthetase 1, mitochondrial	0.023	13.868
ALDH1L1	NM_012190	Aldehyde dehydrogenase 1 family, member L1	0.007	11.772
HMGCS2	NM_005518	3-Hydroxy-3-methylglutaryl-Coenzyme A synthase 2 (mitochondrial)	0.005	8.819
TMPRSS6	NM_153609	Transmembrane protease, serine 6	0.031	7.609
TAT	NM_000353	Tyrosine aminotransferase	0.023	6.929
CYP2D6	NM_000106	Cytochrome P450, family 2, subfamily D, polypeptide 6	0.005	4.932
ACOT12	NM_130767	Acyl-CoA thioesterase 12	0.029	4.353
ADH1C	NM_000669	Alcohol dehydrogenase 1C (class I), γ polypeptide	0.007	4.216
B3GALT1	NM_020981	UDP-Gal:betaGlcNAc β1,3-galactosyltransferase, polypeptide 1	0.031	3.909
PKIB	NM_181795	Protein kinase (cAMP-dependent, catalytic) inhibitor β	0.007	3.462
PI3	NM_002638	Peptidase inhibitor 3, skin-derived	0.044	2.873
KHK	NM_000221	Ketohexokinase (fructokinase)	0.009	2.555
B3GNT7	NM_145236	UDP-GlcNAc:βGal β-1, 3-N-acetylglucosaminyltransferase 7	0.014	2.466

Table IV. Continued.

Gene symbol	Accession number	Gene name	P-value	Fold change
NAGS	NM_153006	N-acetylglutamate synthase	0.029	2.341
ENO2	NM_001975	Enolase 2 (γ, neuronal)	0.007	2.171
C10orf10	NM_007021	Chromosome 10 open reading frame 10	0.031	2.074
HK2	NM_000189	Hexokinase 2	0.033	2.050
Transporter activity				
HPX	NM_000613	Hemopexin	0.005	163.982
FABP1	NM_001443	Fatty acid binding protein 1, liver	0.005	116.798
SLC38A4	NM_018018	Solute carrier family 38, member 4	0.009	6.334
SLCO4A1	NM_016354	Solute carrier organic anion transporter family, member 4A1	0.009	3.035
PAEP	NM_002571	Progestagen-associated endometrial protein	0.038	2.474
The others				
NRN1	NM_016588	Neuritin 1	0.019	2.439
FAM162B	NM_001085480	Family with sequence similarity 162, member B	0.026	2.124
CLEC2B	NM_005127	C-type lectin domain family 2, member B	0.036	2.068
Unknown				
ANKFN1	NM_153228	Ankyrin-repeat and fibronectin type III domain containing 1	0.049	2.023
N/A	AK129542		0.007	3.388
N/A	AW444553		0.039	2.960
LOC100288985	XM_002342826	Hypothetical protein LOC100288985	0.050	2.753
N/A	BF213738		0.039	2.023

P-value, Benjamini-Hochberg false discovery rate of random permutation test; Fold change, ratio of gene expression levels between groups. Gene symbol, accession number, gene name: exported from GeneSpring (from the NCBI databases). FC, fold change; N/A, not available. In each gene ontology functional term, genes were ranked according to fold change (highest to lowest).

(Fig. 3). Genes that were previously reported to be involved in bone metastasis or lung-carcinogenesis were identified in our results, including *FGFR3, TTYH1, LEFTY1, TM4SF4, CRYM, FOLR1, METTL4* and *GUCY1B3*. The *FGFR3* and *TTYH1* genes are already reported to be associated with bone metastasis in breast cancers (16). *TM4SF4* and *CRYM* genes were reported as tumor markers in lung cancer (17-19). *FOLR1* gene was reported to be overexpressed in lung adenocarcinoma (20,21) and has critical involvement in drug resistance (22). *METTL4* gene is known to be related to invasiveness and survival in lung cancer (23), and *GUCY1B3* gene was reported to be involved in osteoclast signaling pathway (24). These findings suggest that those genes may potentially contribute to the bone-preferential metastasis of NSCLC cells.

Discussion

The molecular basis of organ tropism, one of the main characteristics of cancer metastasis, is still largely obscure. It has been documented that different types of cancer produce metastases at preferred secondary sites, depending on organ-susceptibility to specific cells. Stephen Paget proposed the 'seed and soil' theory that the molecular interactions between metastatic cells (seeds) and stromal microenvironment (soil) play critical roles throughout the multi-process of metastasis (25,26). In this study, we used a previously established multi-organ metastasis mouse

model (13), in which cancer cells were inoculated directly into the tail vein that travels to the lungs. Although the tumor cells can be trapped at the lungs as first capillary beds, there were also possibilities that the cells circulate systemically and can reach any organ. Therefore, the analysis of transcriptomic profiles of metastatic lesions in the three organs, bone, lung and liver, can lead to the identification of genetic changes in later steps of the metastasis cascade, when tumor cells have already homed to the specific organ. These changes also reflect the interaction between cancer cells and the local or host cells in the 'microenvironment' of the organ. To form metastatic tumors in a certain organ, cancer cells when homing to this specific organ must interact with the host microenvironment (25-27). To do so, certain molecular programs in cancer cells are activated (25,27). Hence, to elucidate the specific changes of cancer cells in different metastatic organs, we performed microdissection to collect a pure population of cancer cells in metastatic lesions in each type of organ (three organs of five mice, totally 15 lesions), subsequently coupled with DNA microarray analysis. Hierarchical clustering analysis of the 299 organ preferentially expressed genes revealed that they seemed to reflect the organ selectivity of metastatic cells (Fig. 2). In particular, we here focused on genes that were preferentially expressed in bone-metastases.

Among them, we demonstrated that the expression levels of *FGFR3* and *TTYH1* genes were significantly upregulated

A

Bone metastases

Lung metastases

Liver metastases

B

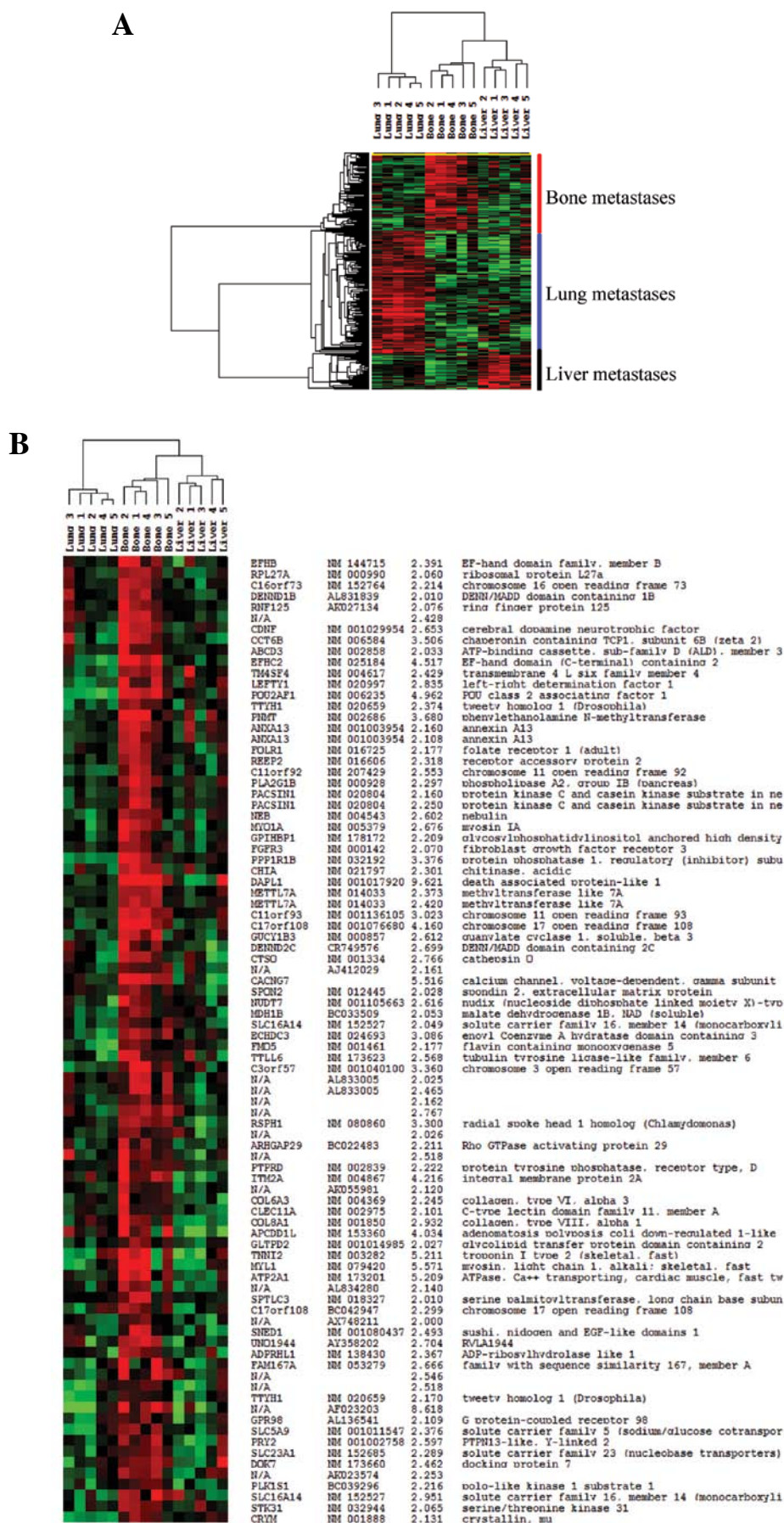| Gene	Accession	Value	Description
EFHB	NM_144715	2.391	EF-hand domain family, member B
RPL27A	NM_000990	2.060	ribosomal protein L27a
C16orf73	NM_152764	2.214	chromosome 16 open reading frame 73
DENND1B	AL831839	2.010	DENN/MADD domain containing 1B
RNF125	AK027134	2.076	ring finger protein 125
N/A		2.428	
CDNF	NM_001029954	2.653	cerebral dopamine neurotrophic factor
CCT6B	NM_006584	3.506	chaperonin containing TCP1, subunit 6B (zeta 2)
ABCD3	NM_002858	2.033	ATP-binding cassette, sub-family D (ALD), member 3
EFHC2	NM_025184	4.517	EF-hand domain (C-terminal) containing 2
TM4SF4	NM_004617	2.429	transmembrane 4 L six family member 4
LEFTY1	NM_020997	2.835	left-right determination factor 1
POU2AF1	NM_006235	4.962	POU class 2 associating factor 1
TTYH1	NM_020659	2.374	tweety homolog 1 (Drosophila)
PNMT	NM_002686	3.680	phenylethanolamine N-methyltransferase
ANXA13	NM_001003954	2.160	annexin A13
ANXA13	NM_001003954	2.108	annexin A13
FOLR1	NM_016725	2.177	folate receptor 1 (adult)
REEP2	NM_016606	2.318	receptor accessory protein 2
C11orf92	NM_207429	2.553	chromosome 11 open reading frame 92
PLA2G1B	NM_000928	2.297	phospholipase A2, group IB (pancreas)
PACSIN1	NM_020804	2.160	protein kinase C and casein kinase substrate in ne
PACSIN1	NM_020804	2.250	protein kinase C and casein kinase substrate in ne
NEB	NM_004543	2.602	nebulin
MYO1A	NM_005379	2.676	myosin IA
GPIHBP1	NM_178172	2.209	glycosylphosphatidylinositol anchored high density
FGFR3	NM_000142	2.070	fibroblast growth factor receptor 3
PPP1R1B	NM_032192	3.376	protein phosphatase 1, regulatory (inhibitor) subu
CHIA	NM_021797	2.301	chitinase, acidic
DAPL1	NM_001017920	9.621	death associated protein-like 1
METTL7A	NM_014033	2.373	methyltransferase like 7A
METTL7A	NM_014033	2.420	methyltransferase like 7A
C11orf93	NM_001136105	3.023	chromosome 11 open reading frame 93
C17orf108	NM_001076680	4.160	chromosome 17 open reading frame 108
GUCY1B3	NM_000857	2.612	guanylate cyclase 1, soluble, beta 3
DENND2C	CR749576	2.699	DENN/MADD domain containing 2C
CTSO	NM_001334	2.766	cathepsin O
N/A	AJ412029	2.161	
CACNG7		5.516	calcium channel, voltage-dependent, gamma subunit
SPON2	NM_012445	2.028	spondin 2, extracellular matrix protein
NUDT7	NM_001105663	2.616	nudix (nucleoside diphosphate linked moiety X)-typ
MDH1B	BC033509	2.053	malate dehydrogenase 1B, NAD (soluble)
SLC16A14	NM_152527	2.049	solute carrier family 16, member 14 (monocarboxyli
ECHDC3	NM_024693	3.086	enoyl Coenzyme A hydratase domain containing 3
FMO5	NM_001461	2.177	flavin containing monooxygenase 5
TTLL6	NM_173623	2.568	tubulin tyrosine ligase-like family, member 6
C3orf57	NM_001040100	3.360	chromosome 3 open reading frame 57
N/A	AL833005	2.025	
N/A	AL833005	2.465	
N/A		2.162	
N/A		2.767	
RSPH1	NM_080860	3.300	radial spoke head 1 homolog (Chlamydomonas)
N/A		2.026	
ARHGAP29	BC022483	2.211	Rho GTPase activating protein 29
N/A		2.518	
PTPRD	NM_002839	2.222	protein tyrosine phosphatase, receptor type, D
ITM2A	NM_004867	4.216	integral membrane protein 2A
N/A	AK055981	2.120	
COL6A3	NM_004369	2.245	collagen, type VI, alpha 3
CLEC11A	NM_002975	2.101	C-type lectin domain family 11, member A
COL8A1	NM_001850	2.932	collagen, type VIII, alpha 1
APCDD1L	NM_153360	4.034	adenomatosis polyposis coli down-regulated 1-like
GLTPD2	NM_001014985	2.027	glycolipid transfer protein domain containing 2
TNNI2	NM_003282	5.211	troponin I type 2 (skeletal, fast)
MYL1	NM_079420	5.571	myosin, light chain 1, alkali; skeletal, fast
ATP2A1	NM_173201	5.209	ATPase, Ca++ transporting, cardiac muscle, fast tw
N/A	AL834280	2.140	
SPTLC3	NM_018327	2.010	serine palmitoyltransferase, long chain base subun
C17orf108	BC042947	2.299	chromosome 17 open reading frame 108
N/A	AX748211	2.000	
SNED1	NM_001080437	2.493	sushi, nidogen and EGF-like domains 1
UNQ1944	AY358202	2.704	RVLA1944
ADPRHL1	NM_138430	2.367	ADP-ribosylhydrolase like 1
FAM167A	NM_053279	2.666	family with sequence similarity 167, member A
N/A		2.546	
N/A		2.518	
TTYH1	NM_020659	2.170	tweety homolog 1 (Drosophila)
N/A	AF023203	8.618	
GPR98	AL136541	2.109	G protein-coupled receptor 98
SLC5A9	NM_001011547	2.376	solute carrier family 5 (sodium/glucose cotranspor
PRY2	NM_001002758	2.597	PTPN13-like, Y-linked 2
SLC23A1	NM_152685	2.289	solute carrier family 23 (nucleobase transporters)
DOK7	NM_173660	2.462	docking protein 7
N/A	AK023574	2.253	
PLK1S1	BC039296	2.216	polo-like kinase 1 substrate 1
SLC16A14	NM_152527	2.951	solute carrier family 16, member 14 (monocarboxyli
STK31	NM_032944	2.065	serine/threonine kinase 31
CRYM	NM_001888	2.131	crystallin, mu

Figure 2. Hierarchical cluster analysis of 15 metastatic lesions. (A) Dendrogram showing the highly expressed genes in metastases in the bone, lung and liver. Total: 299 genes. (B) A section of the above dendrogram showing genes preferentially expressed in bone metastases. In the dendrograms, row represents a single gene; column represents the metastatic lesion; and color: red, green or black indicates high, low or unchanged expression level, respectively, of corresponding gene relative to the mean.
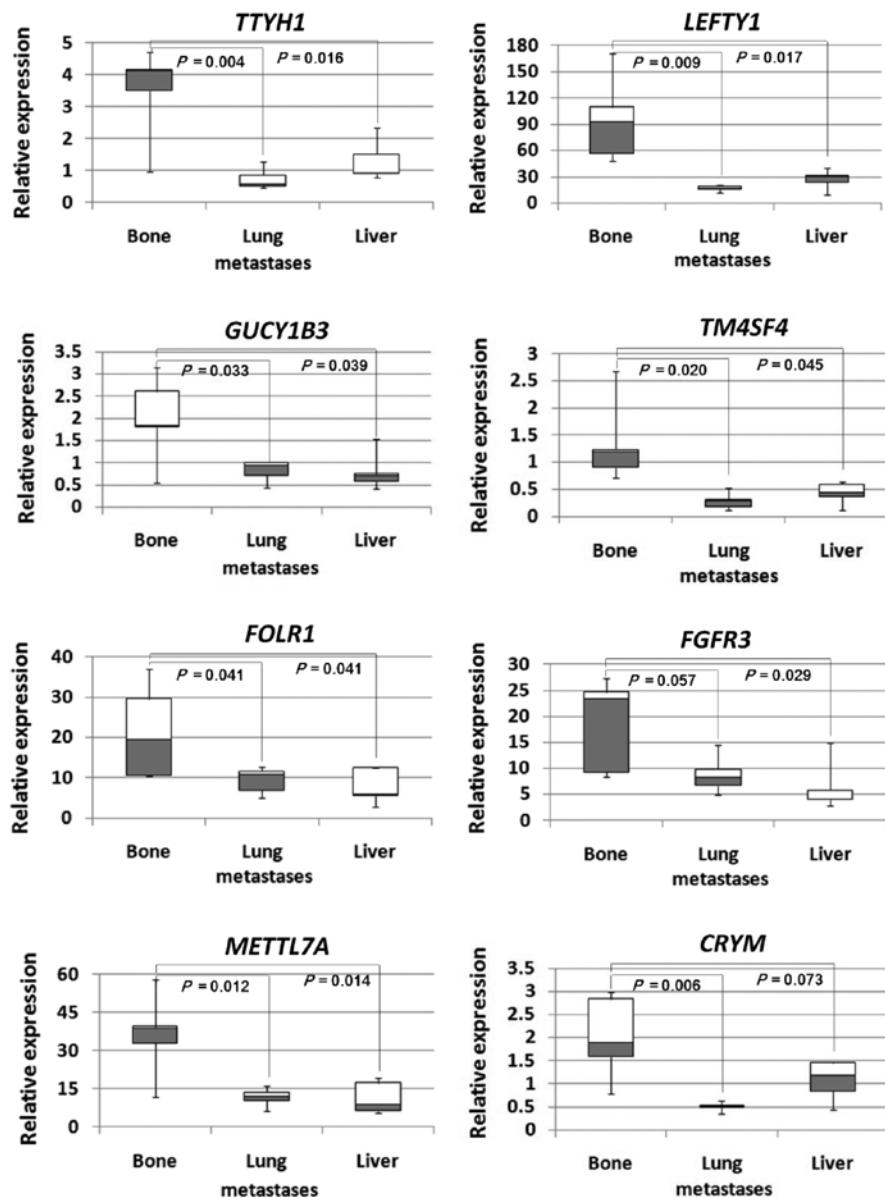
Figure 3. Box plots showing expression levels of eight selected genes in bone, lung and liver metastatic legions. *GAPDH* was used for normalization. Data are expressed as the fold increase over ACC-LC319/bone2 original cells (set at 1.0), and represent the mean ± SE of three independent experiments.

in bone metastasis compared with metastasis in lung or liver. These genes have been previously reported to be upregulated in human breast cancer bone metastasis in clinical specimen (16). Smid *et al* reported analysis of expression profiling in 107 human breast cancer patients who had relapse in bone or other sites in the body, and identified a panel of 69 genes that were upregulated in bone relapse, which included *FGFR3* and *TTYH1* (16).

FGFR3, encoding a receptor tyrosine kinase for fibroblast growth factor, was reported to be overexpressed in ~15-20% cases of myeloma, or constituvely activated due to mutations in most of bladder cancers and other solid tumors, including lung cancers. Fibroblast growth factors (FGF) are bone-derived factors abundant in the bone environment (6,26), therefore it is reasonable that lung cancer cells highly expressing FGFR3 might be more selectively colonized in bone than in lung or liver. In addition, the FGF-FGFR3 signaling pathway via Ras-MAPK and PI3K in cancer cells may lead to enhanced

cell proliferation and migration (reviewed in refs. 28 and 29). TTYH1, an endoplasmic-localized protein, was reported to be a Ca^{2+}-binding protein playing critical roles in mitosis and cell proliferation (30). This molecule may therefore be essential for the cancer cells homing to the bone, and may contribute to the growth advantage of the metastatic tumors in the bone. *LEFTY1* (also known as *LEFTY-B*), another promising target gene in the bone metastases profile, was confirmed to be significantly upregulated in bone metastasis. LEFTY1 was reported to be a secreted molecule of the TGF-β superfamily involved in the Nodal signaling pathway, and a marker of the stemness of cells (31-33), and to contribute to the remodeling process of the extracellular matrix (34). In contrast, LEFTY1 also plays an important role as an inhibitor of Nodal, a crucial component involved in metastatic melanoma cells, in a negative feedback mechanism (reviewed in ref. 33).

Recently, it was reported that cancer stem cells possess tumorigenic, invasive and migratory characteristics (25,27), and

tumor cell plasticity (33). These individual lines of evidence suggest that LEFTY1 may be involved in metastasis. Moreover, *GUCY1B3*, encoding an enzyme that catalyzes the conversion of GTP to cyclic GMP, is well-known to be involved in the pathway of nitride oxide signaling, which is one of the major post differentiation pathways in the osteoclast (24). It is reported that the enhancement of a soluble form of GUCY1B3 led to the activation of the osteoclasts in the osteolytic bone metastasis process. Moreover, this protein enhances tumor growth of glioma (35) and angiogenesis in both glioma and chorioallantoic membrane (35,36), and plays paradoxical roles in the proliferation of cancer cells (37), suggesting that GUCY1B3 could be involved in bone metastasis.

Furthermore, among the genes highly expressed in lung metastasis, we identified genes encoding surfactant protein C and D (SFTPC and SFTPD: 192- and 95-fold changes, respectively). Serum levels of SFTPC and SFTPD were previously reported to be elevated in mice with lung tumors (38,39). In humans, a research on lung adenocarcinoma showed the upregulation of *SFTPC* and *SFTPD*, especially *SFTPD*, in lymph node metastatic lesions (17 in 23 cases of metastases or micrometastases) (40). Although specific role(s) of these molecules in lung metastasis are not characterized so far, our findings raise the possibilities that SFTPC and SFTPD proteins regulate the process of metastasis in general, or specifically, lung colonization, of the cancer cells in this multi-organ metastasis mouse model. Moreover, Claudin-18 (CLDN18), a tight junction molecule, was upregulated ~21-fold in lung metastases as compared with metastases in other organs. A recent immunotherapeutic strategy using auto-antibody against CLDN18 shows that the formation of pulmonary metastasis was significantly reduced in mice inoculated intravenously with colon cancer cells (41), suggesting that CLDN18 could be a specific molecule for controlling metastasis, especially lung metastases. In addition, Dickkopf-1 (DKK1), a secreted protein that negatively regulates the Wnt signaling pathway, was upregulated 11-fold in lung metastases. It has been reported that DKK1 is a serologic and prognostic biomarker for lung cancers (42,43).

Finally, we focused on genes that were rank-ordered among genes that were preferentially expressed in liver metastasis, namely hemopexin (HPX) and vitronectin (VTN). HPX and VTN proteins belong to the hemopexin superfamily which includes matrix metalloproteinases (MMPs). HPX which is highly expressed in the liver binds to hemes and negates the toxic effect of hemes. It is remarkable that there are hundreds of proteins, including MMPs, containing one or several motifs that structurally and functionally resemble parts of the HPX protein (review in ref. 44). A latest report shows that small-molecule compounds that selectively target the hemopexin domain of MMP-9 can control tumor growth and inhibit lung metastasis in breast cancer xenograft model in mice (45). Moreover, VTN, an extracellular protein that interacts with many integrins, is also expressed highly in the liver, and was previously reported to be upregulated in primary hepatocellular carcinoma (46), or liver metastases from colorectal cancer (46,47) and neuroblastoma (48).

Thus, we identified a dozen potential metastasis-related molecules including other unknown functional molecules. However, relating to bone metastasis, there were no overlapping genes compared with previous report in SCLC (using SBC-5

cell line) (13). This may reflect the fact that there are distinctive biologic processes involved in SCLC or NSCLC bone metastasis, although in both cases bone metastatic lesions were of same osteolytic phenotype. Vicent *et al* reported a lung cancer bone metastasis gene profile using NSCLC (NCI-H460, a large cell carcinoma cell line), by comparing the transcriptomes of the sublines possessing highly bone metastatic ability and the parental cell lines (12). However, none of the genes in their data were identified in our bone metastasis gene profile. This discrepancy on microarray data may be due to several factors. In this study, we focused on lung cancer bone metastases from NSCLC (adenocarcinoma, ~60-70% of non-resectable NSCLC), not SCLC (4). In fact, SCLC consists of only ~15-20% of lung cancers, whereas NSCLC consists of 80-85%, and the natural course as well as the molecular basis of SCLC is quite distinct from NSCLC (2,4). The above evidence suggests that there were differences in the biology of bone metastases in NSCLC in comparison with SCLC.

In conclusion, through a human NSCLC cell line with enhanced bone metastasis ability in a multi-organ metastasis mouse model coupled with microarray analysis, we identified dozens of genes which were potentially involved in metastases to the bone, lung, and liver. However, it will be necessary to perform further functional analyses using gain- or loss-of-function approaches in mouse models and validation in human clinical samples. Our findings should be helpful for better understanding of molecular aspects of the metastatic process in different microenvironments, especially in bone metastases, and could lead to molecular target-based anticancer drugs and prevention of metastasis.

References

1. Jemal A, Bray F, Center MM, *et al*: Global cancer statistics. CA Cancer J Clin 61: 69-90, 2011 (Erratum in CA Cancer J Clin 61: 134, 2011).
2. Herbst RS, Heymach JV and Lippman SM: Lung cancer. N Engl J Med 359: 1367-1380, 2008.
3. Al Husaini H, Wheatley-Price P, Clemons M, *et al*: Prevention and management of bone metastases in lung cancer: a review. J Thorac Oncol 4: 251-259, 2009.
4. Stenbygaard LE, Sørensen JB, Larsen H, *et al*: Metastatic pattern in non-resectable non-small cell lung cancer. Acta Oncol 38: 993-998, 1999.
5. Sone S and Yano S: Molecular pathogenesis and its therapeutic modalities of lung cancer metastasis to bone. Cancer Metastasis Rev 26: 685-689, 2007.
6. Roodman GD: Mechanisms of bone metastasis. N Engl J Med 350: 1655-1664, 2004.
7. Mundy GR: Metastasis to bone: causes, consequences and therapeutic opportunities. Nat Rev Cancer 2: 584-593, 2002.
8. Ibrahim T, Flamini E, Mercatali L, *et al*: Pathogenesis of osteoblastic bone metastases from prostate cancer. Cancer 116: 1406-1418, 2010 (Erratum in: Cancer 116: 2503, 2010).
9. Weilbaecher KN, Guise TA and McCauley LK: Cancer to bone: a fatal attraction. Nat Rev Cancer 11: 411-425, 2011.

10. Rose AA and Siegel PM: Emerging therapeutic targets in breast cancer bone metastasis. Future Oncol 6: 55-74, 2010.
11. Kakiuchi S, Daigo Y, Tsunoda T, et al: Genome-wide analysis of organ-preferential metastasis of human small cell lung cancer in mice. Mol Cancer Res 1: 485-499, 2003.
12. Vicent S, Luis-Ravelo D, Antón I, et al: A novel lung cancer signature mediates metastatic bone colonization by a dual mechanism. Cancer Res 68: 2275-2285, 2008.
13. Otsuka S, Hanibuchi M, Ikuta K, et al: A bone metastasis model with osteolytic and osteoblastic properties of human lung cancer ACC-LC-319/bone2 in natural killer cell-depleted severe combined immunodeficient mice. Oncol Res 17: 581-591, 2009.
14. Eisen MB, Spellman PT, Brown PO, et al: Cluster analysis and display of genome-wide expression patterns. Proc Natl Acad Sci USA 95: 14863-14868, 1998.
15. de Hoon MJL, Imoto S, Nolan J, et al: Open source clustering software. Bioinformatics 20: 1453-1454, 2004.
16. Smid M, Wang Y, Klijn JG, et al: Genes associated with breast cancer metastatic to bone. J Clin Oncol 24: 2261-2267, 2006.
17. Wang KK, Liu N, Radulovich N, et al: Novel candidate tumor marker genes for lung adenocarcinoma. Oncogene 21: 7598-7604, 2002.
18. Chong IW, Chang MY, Chang HC, et al: Great potential of a panel of multiple hMTH1, SPD, ITGA11 and COL11A1 markers for diagnosis of patients with non-small cell lung cancer. Oncol Rep 16: 981-988, 2006.
19. Nakamura N, Kobayashi K, Nakamoto M, et al: Identification of tumor markers and differentiation markers for molecular diagnosis of lung adenocarcinoma. Oncogene 25: 4245-4255, 2006.
20. Iwakiri S, Sonobe M, Nagai S, et al: Expression status of folate receptor alpha is significantly correlated with prognosis in non-small-cell lung cancers. Ann Surg Oncol 15: 889-899, 2008.
21. Jin M, Kawakami K, Fukui Y, et al: Different histological types of non-small cell lung cancer have distinct folate and DNA methylation levels. Cancer Sci 100: 2325-2330, 2009.
22. Sánchez-del-Campo L, Montenegro MF, Cabezas-Herrera J, et al: The critical role of alpha-folate receptor in the resistance of melanoma to methotrexate. Pigment Cell Melanoma Res 22: 588-600, 2009.
23. Liu R, Wang X, Chen GY, et al: The prognostic role of a gene signature from tumorigenic breast-cancer cells. N Engl J Med 356: 217-226, 2007.
24. Blair HC, Robinson LJ and Zaidi M: Osteoclast signaling pathways. Biochem Biophys Res Commun 328: 728-738, 2005.
25. Talmadge JE and Fidler IJ: AACR centennial series: the biology of cancer metastasis: historical perspective. Cancer Res 70: 5649-5669, 2010.
26. Casimiro S, Guise TA and Chirgwin J: The critical role of the bone microenvironment in cancer metastases. Mol Cell Endocrinol 310: 71-81, 2009.
27. Hanahan D and Weinberg RA: Hallmarks of cancer: the next generation. Cell 144: 646-674, 2011.
28. Haugsten EM, Wiedlocha A, Olsnes S, et al: Roles of fibroblast growth factor receptors in carcinogenesis. Mol Cancer Res 8: 1439-1452, 2010.
29. L'Hôte CG and Knowles MA: Cell responses to FGFR3 signalling: growth, differentiation and apoptosis. Exp Cell Res 304: 417-431, 2005.
30. Kumada T, Yamanaka Y, Kitano A, et al: Ttyh1, a Ca^{2+}-binding protein localized to the endoplasmic reticulum, is required for early embryonic development. Dev Dyn 239: 2233-4225, 2010.
31. Besser D: Expression of Nodal, Lefty-A, and Lefty-B in undifferentiated human embryonic stem cells requires activation of Smad2/3. J Biol Chem 279: 45076-45084, 2004.
32. Dvash T, Sharon N, Yanuka O, et al: Molecular analysis of LEFTY-expressing cells in early human embryoid bodies. Stem Cells 25: 465-472, 2007.
33. Hendrix MJ, Seftor EA, Seftor RE, et al: Reprogramming metastatic tumour cells with embryonic microenvironments. Nat Rev Cancer 7: 246-255, 2007.
34. Mason JM, Xu HP, Rao SK, et al: Lefty contributes to the remodeling of extracellular matrix by inhibition of connective tissue growth factor and collagen mRNA expression and increased proteolytic activity in a fibrosarcoma model. J Biol Chem 277: 407-415, 2002.
35. Saino M, Maruyama T, Sekiya T, et al: Inhibition of angiogenesis in human glioma cell lines by antisense RNA from the soluble guanylate cyclase genes, GUCY1A3 and GUCY1B3. Oncol Rep 12: 47-52, 2004.
36. Pyriochou A, Beis D, Koika V, et al: Soluble guanylyl cyclase activation promotes angiogenesis. Pharmacol Exp Ther 319: 663-671, 2006.
37. Mujoo K, Sharin VG, Martin E, et al: Role of soluble guanylyl cyclase-cyclic GMP signaling in tumor cell proliferation. Nitric Oxide 22: 43-50, 2010.
38. Mason RJ, Kalina M, Nielsen LD, et al: Surfactant protein C expression in urethane-induced murine pulmonary tumors. Am J Pathol 156: 175-182, 2000.
39. Zhang F, Pao W, Umphress S, et al: Serum levels of surfactant protein D are increased in mice with lung tumors. Chest 125 (Suppl 5): 109, 2004.
40. Betz C, Papadopoulos T, Buchwald J, et al: Surfactant protein gene expression in metastatic and micrometastatic pulmonary adenocarcinomas and other non-small cell lung carcinomas: detection by reverse transcriptase-polymerase chain reaction. Cancer Res 55: 4283-4286, 1995.
41. Klamp T, Schumacher J, Huber G, et al: Highly specific auto-antibodies against claudin-18 isoform 2 induced by a chimeric HBcAg virus-like particle vaccine kill tumor cells and inhibit the growth of lung metastases. Cancer Res 71: 516-527, 2011.
42. Yamabuki T, Takano A, Hayama S, et al: Dikkopf-1 as a novel serologic and prognostic biomarker for lung and esophageal carcinomas. Cancer Res 67: 2517-2525, 2007.
43. Sheng SL, Huang G, Yu B, et al: Clinical significance and prognostic value of serum Dickkopf-1 concentrations in patients with lung cancer. Clin Chem 55: 1656-1664, 2009.
44. Piccard H, Van den Steen PE and Opdenakker G: Hemopexin domains as multifunctional liganding modules in matrix metallo-proteinases and other proteins. J Leukoc Biol 81: 870-892, 2007.
45. Dufour A, Sampson NS, Li J, et al: Small-molecule anticancer compounds selectively target the hemopexin domain of matrix metalloproteinase-9. Cancer Res 71: 4977-4988, 2011.
46. Edwards S, Lalor PF, Tuncer C, et al: Vitronectin in human hepatic tumours contributes to the recruitment of lymphocytes in αvβ3-independent manner. Br J Cancer 95: 1545-1554, 2006.
47. Yoshioka T, Nishikawa Y, Ito R, et al: Significance of integrin αvβ5 and erbB3 in enhanced cell migration and liver metastasis of colon carcinomas stimulated by hepatocyte-derived heregulin. Cancer Sci 101: 2011-2018, 2010.
48. Kuwashima N: Organ-specific adhesion of neuroblastoma cells in vitro: correlation with their hepatic metastasis potential. J Pediatr Surg 32: 546-551, 1997.